




# The Use of TEMPO-oxidized Nanofibrillated Cellulose as Anode Binder for Lithium-ion Batteries

Soojin Kwon <sup>a,b</sup>, Ju Yoon Moon,<sup>c</sup> Sang Yun Kim <sup>d</sup>, and Kyudeok Oh <sup>c,d,\*</sup>

Expansion of the anode coating layer during lithium-ion battery charging and discharging is of significant concern because it can delaminate or break the coating layer, thus critically affecting battery lifespan and the efficiency, especially in silicon-based electrodes. Therefore, control of expansion and improvement of the mechanical properties of the anode layer are essential. Nanofibrillated cellulose (NFC) exhibits excellent network-forming and mechanical properties and have been extensively researched in terms of high-value applications. This study aims to enhance the rheological and mechanical properties of conventional anode layers by using TEMPO-oxidized NFC (TNFC) as the binder. Anode coating processability was investigated through rheological properties, and the interaction mechanisms between TNFC and electrode graphite were explored. Performance changes were examined using tensile and peel tests to assess adhesion between the electrode and copper foil. The tensile properties of an anode with TNFC improved dramatically. The use of TNFC alone as binder reduced the electrode abrasion resistance to copper foil, but this can be countered by combining TNFC with a traditional SBR binder. This study thus highlights the potential of TNFC as novel renewable binders for anodes.

DOI: 10.15376/biores.20.2.3732-3748

*Keywords:* Cellulose nanofibrils; Lithium-ion battery; Environmentally friendly binder; Anode slurry

*Contact information:* a: Department of Environmental Materials Science, Gyeongsang National University, Jinju 52828, South Korea; b: Institute of Agriculture & Life Science, Gyeongsang National University, Jinju, 52828, South Korea; c: Program in Environmental Materials Science, Department of Agriculture, Forestry and Bioresources, College of Agriculture and Life Sciences, Seoul National University, Seoul 08826, South Korea; d: Research Institute of Agriculture and Life Sciences, Seoul National University, Seoul 08826, South Korea; \*Corresponding author: kyudeok.oh@snu.ac.kr

## INTRODUCTION

Lithium-ion batteries (LIBs), which are chemical batteries, are competitive renewable energy storage systems not only for electric vehicles (EVs) but also for various electronics, including laptops and smartphones, among others (El Kharbachi *et al.* 2020; Wassiliadis *et al.* 2021). The demand for safe and efficient EV batteries has greatly increased and will continue to do so, but significant limitations include battery safety and lifespan, which cause consumer concern.

A typical LIB has four main components: cathodic and anodic electrodes, electrolytes, and a separator membrane. During charging, lithium ions move from the cathode through the separator membrane and then become attached to the anode. The ions move back to the cathode during discharge. Therefore, electrode structures and properties that facilitate efficient lithiation and delithiation are critical in terms of battery efficiency and lifespan. The properties of electrodes are ultimately determined by the interactions

among components in anode slurries and the microstructures formed during manufacturing, *i.e.*, from the dispersion of raw materials to drying and calendaring (Lim *et al.* 2015; Gordon *et al.* 2020a; Dufficy *et al.* 2021; Kitamura *et al.* 2022). Thus, both the raw material properties and manufacturing control must be considered to improve LIBs.

Anodes are typically composed of anodic materials, such as graphite, and binders, such as styrene–butadiene rubber (SBR) and carboxymethyl cellulose (CMC). Binders play crucial roles in anode structure maintenance and prevention of layer failures. Binders ensure adhesion between individual anodic materials, and between anodic materials and foils. During charging and discharging, the anode layer inevitably expands and contracts with lithiation and delithiation (Lee *et al.* 2003; Nitta *et al.* 2015; Schweidler *et al.* 2018). Such expansion can damage the layer and trigger local layer detachment from the copper foil, reducing long-term battery efficiency and stability. Hence, improving binder performance to reduce the dimensional stress caused by charging and discharging, to make the system better tolerate expansion, and to maintain the anode's structural integrity is essential to make LIBs more efficient and stable. Additionally, achieving a uniform structure with an even distribution of graphite particles is critical for minimizing volumetric expansion (Park *et al.* 2019).

CMC, a typical binder, is a cellulose derivative with carboxymethyl functional groups. When used in combination with SBR, CMC can enhance the mechanical stability and conductivity of the electrode compared to an SBR-only binder system (Buqa *et al.* 2006). The behavior of anode slurries and the electrode properties differ depending on the CMC molecular weight (MW) and degree of substitution (DS). For example, high-MW, low-DS CMC enhances anode slurry dispersion by improving absorption to graphite particles (Gordon *et al.* 2020b), whereas high-MW, high-DS CMC can improve the cycling performance of the electrode (Hochgatterer *et al.* 2008). While CMC's stiffness and strong interaction with anode materials contribute to the mechanical stability of the battery (Sen and Mitra 2013; Qiu *et al.* 2014), these same properties can also reduce the flexibility of the electrode layer (Qian *et al.* 2012).

Nanofibrillated cellulose (NFC; also called cellulose nanofibril), which are mechanically and/or chemically fibrillated cellulose, have higher aspect ratios and larger specific surface areas similar to high-MW/low-DS CMC, and may thus interact better with anode materials. NFC generally exhibits high moduli and superior mechanical properties (Iwamoto *et al.* 2009). Superior performance of NFC in slurries, similar to that in anodic slurries, has been reported (Dimic-Misic *et al.* 2013; Rautkoski *et al.* 2015; Salo *et al.* 2015; Oh *et al.* 2017). Recently, a limited number of studies have explored the application of NFC as binders in LIBs, showing improved cycling and mechanical performance compared to conventional binder systems, such as polyvinylidene fluoride (PVDF) or CMC/SBR binder systems (Lu *et al.* 2017; Nirmale *et al.* 2017; Françon *et al.* 2022). In most studies, TEMPO-oxidized nanofibrillated cellulose (TNFC) has been selected as the NFC binder. Its higher surface charge, resulting from the TEMPO oxidation process, demonstrates promising properties as an electrode binder. For example, Lu *et al.* (2017) highlighted the potential of TNFC as a binder for flexible LiFePO<sub>4</sub> electrodes, illustrating the impact of the manufacturing process and TNFC charge density on mechanical and electrochemical properties. However, the electrodes in this study were fabricated using a filtration process to create paper-based electrodes, differing from the conventional coating processes typically used in electrode manufacturing. Another study investigated the positive effects of TNFC in an anode slurry coating system compared to the CMC/SBR binder system, confirming improvements in shear stress and specific capacities (Françon *et al.* 2022).

Nevertheless, further investigation is needed into the bonding properties and mechanical behavior of free-standing composites to fully understand the potential of NFC-based electrodes. Moreover, comprehensive rheological tests would be beneficial for understanding NFC behavior as a binder in anode slurries.

Therefore, this study investigated the effects of replacing the SBR/CMC binder system with TNFC on the rheological properties of anode slurries and the mechanical properties, including adhesion of the anode layer to the copper surface and the tensile properties of anodes with TNFC binders. Advantages of NFC as an anode binder were highlighted, suggesting future research directions and practical applications.

## EXPERIMENTAL

### Materials

Graphite (SG-BH8; Ito Graphite Co. Ltd., Japan) served as the anode material. This natural graphite has a D50 diameter of 8.7  $\mu\text{m}$  (Fig. 1 (a–b)).

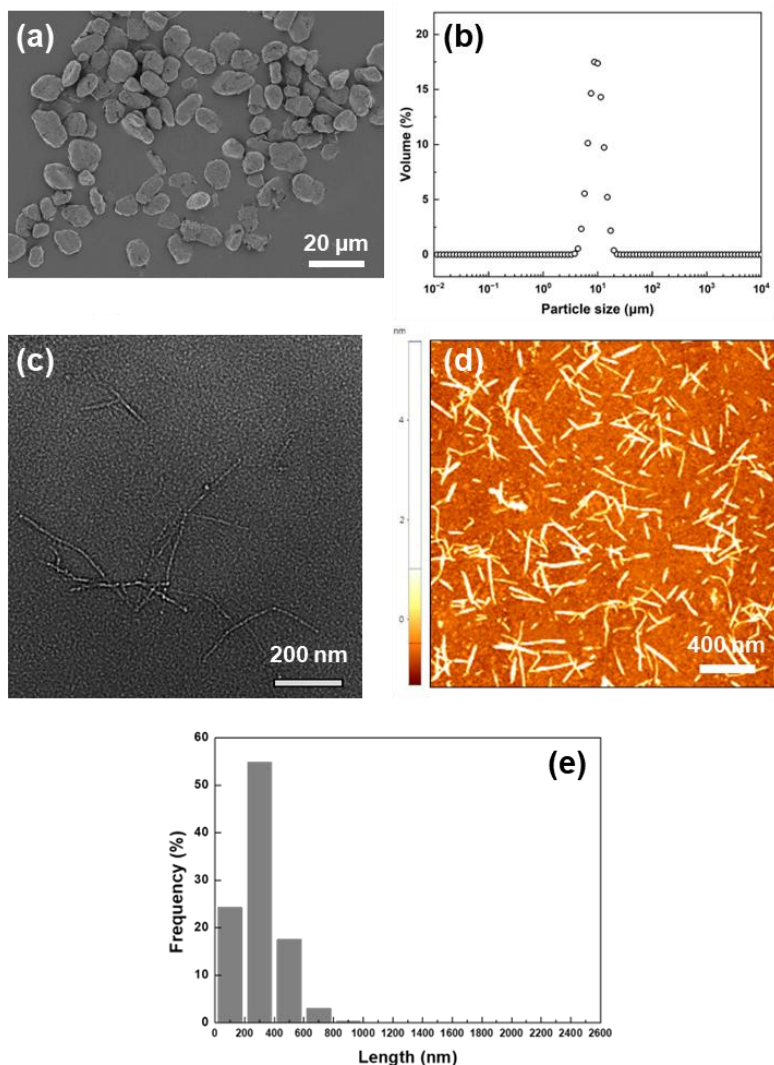


**Fig. 1.** Sample morphologies: (a) SEM image of graphite, (b) graphite particle size distribution, (c) SEM image of TNFC, (d) AFM image of TNFC, and (e) fiber length of TNFC from (c)

Conventional SBR latex was provided by LG Energy Solution (Korea) and used as a reference binder. CMC (MW 250 kDa, DS 0.9) was purchased from Sigma-Aldrich (USA). TEMPO-oxidized NFC (TNFC) was supplied by Hansol Paper Co. (Korea). The average fiber width and length were 2.8 and 364.7 nm, respectively. The fiber width was measured *via* atomic force microscopy (AFM) in non-contact mode (XE-100, PSIA, Korea), and the fiber length was obtained *via* scanning electron microscopy (SEM; JEM-2100PLUS; JEOL, Japan) (Fig. 1 (c–e)).

#### Preparation of anode slurries

The compositions of all slurries are shown in Table 1. All slurries were prepared using the same method: graphite and TNFC were added to deionized water and dispersed with a homogenizer for 5 min, followed by 10 min of stirring.

**Table 1.** Anode Slurry Composition by TNFC Content

|                          | Ref. | TNFC<br>0% | TNFC<br>0.05% | TNFC<br>0.1% | TNFC<br>0.15% | TNFC<br>0.2% | TNFC<br>0.5% | TNFC<br>1.0% | TNFC<br>1.5% | TNFC<br>2.0% | TNFC<br>2.5% |
|--------------------------|------|------------|---------------|--------------|---------------|--------------|--------------|--------------|--------------|--------------|--------------|
| Solids<br>content<br>(%) | 50   |            |               |              |               |              |              |              |              |              |              |
| Graphite<br>(%)          | 97   | 100        | 99.95         | 99.9         | 99.85         | 99.8         | 99.5         | 99           | 98.5         | 98           | 97.5         |
| NFC<br>(%)               | -    | -          | 0.05          | 0.1          | 0.15          | 0.2          | 0.5          | 1.0          | 1.5          | 2.0          | 2.5          |
| CMC<br>(%)               | 1    | -          | -             | -            | -             | -            | -            | -            | -            | -            | -            |
| SBR<br>(%)               | 2    | -          | -             | -            | -             | -            | -            | -            | -            | -            | -            |

#### Sample preparation for 90° peel tests

Anode layers for peel tests were coated onto copper foil using an automatic coater (KP-3000V, Kipae, Korea) and an applicator with a 400- $\mu$ m gap (Fig. 2). After coating, each layer was dried at 60 °C for 30 min.

#### Free-standing composites for tensile tests

Free-standing composites for tensile tests were manufactured using the mold casting method shown in Fig. 3. The mold (60 × 80 × 0.8 mm) was placed on glass with a release film to facilitate easy composite separation from the mold. All specimens were then cut to 10 × 50 mm using a paper guillotine cutter. The specimen thickness was 0.4 to 0.6  $\mu$ m.

## Characterization

#### Rheological properties of anode slurries

The rheological properties of anode slurries were investigated using a rotational rheometer (MCR 302e Modular Compact Rheometer; Anton Paar, Austria) with a Couette geometry (CC27; working gap 5.7 mm). All measurements were conducted at room temperature (25 °C). Viscosity was measured over a shear rate range from 0.01 to 1,000  $s^{-1}$  in shear rate-controlled mode. Oscillatory tests, including amplitude and frequency

sweep measurements, were performed to analyze the viscoelastic properties. The storage ( $G'$ ) and loss ( $G''$ ) moduli were measured as functions of the shear strain (0.001 to 1,000%) and frequency (0.1 to 100 rad/s). Binder distributions within slurries were explored using an optical microscope (BX51; Olympus, Japan).

#### *Mechanical tests*

The 90° peel test analyzed adhesion of the anode layer to the copper foil; a Universal Testing Machine (UTM; 594; Instron, USA) (Fig. 2) was employed along with a 50-N load cell. The anode layer was pulled vertically from the copper foil at 100 mm/min commencing at a grip distance of 30 mm. After the peel test, the residual anode layer on the copper foil was examined both visually and under an optical microscope.

The strength of anode free-standing composites was determined *via* tensile testing using the instrument employed for the peel test. A 1-kN load cell was used; the test speed was 0.1 mm/min, and the test span was 20 mm.

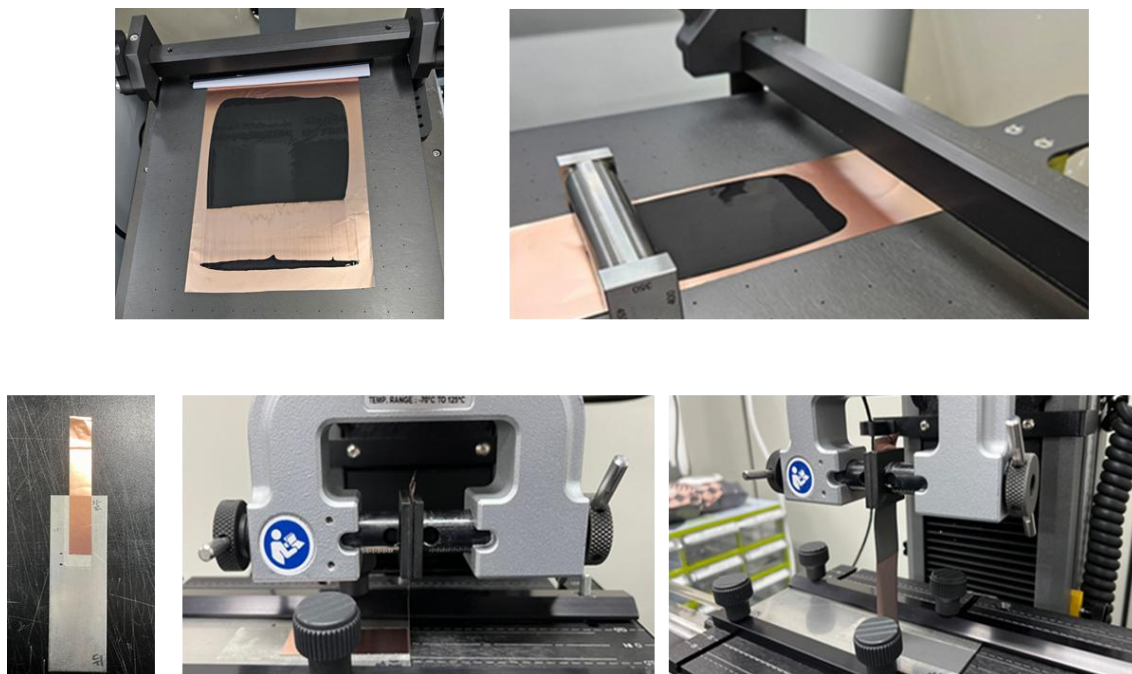


**Fig. 2.** Preparation of an anode layer for the 90° peel strength test and the UTM setup



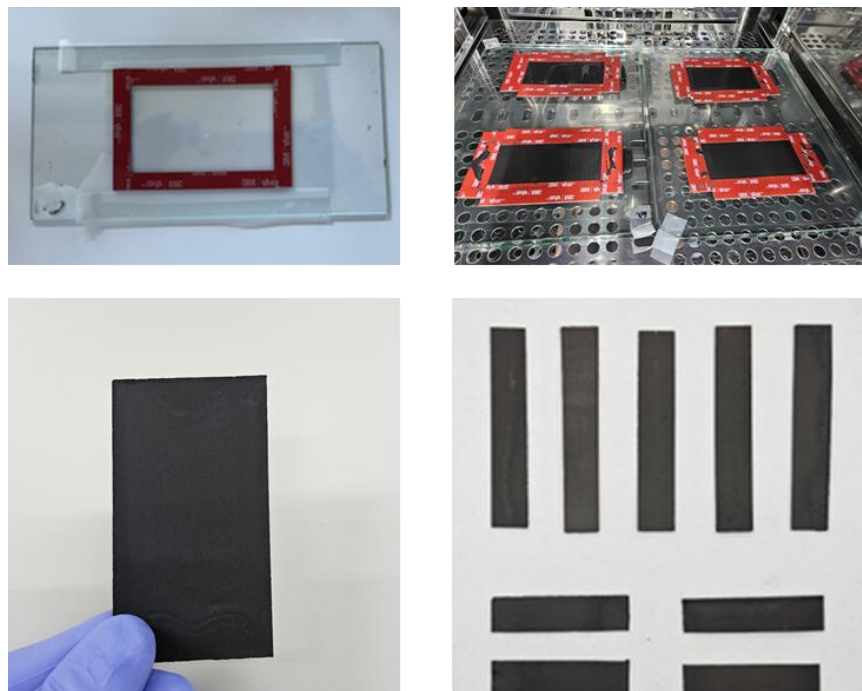


**Fig. 3.** Preparation of free-standing composites for the tensile test employing the UTM

## RESULTS AND DISCUSSION

In the current study, the effect of TNFC as an anode binder on anode slurry and composite was investigated. Rheological and mechanical properties were examined to determine whether TNFC improved processability and anode binder performance. Additionally, the interaction between TNFC and graphite in the anode slurries was considered based on rheological analysis and optical microscopy.

### Rheological Properties of Anode Slurries with NFC

The effect of TNFC on anode slurry viscosity was investigated using 10 TNFC concentrations (Table 1). The viscosities of slurries with different TNFC and CMC levels were measured for comparison (Fig. 4). All slurries exhibited shear-thinning behavior, but the anode slurries with TNFC showed higher viscosities compared to those with CMC, consistent with previous findings (Françon *et al.* 2022). Given that the viscosity of cellulose nanofibers is positively correlated with their aspect ratio (Iwamoto *et al.* 2014), the higher aspect ratio of TNFC compared to CMC makes TNFC more effective as thickeners. The viscosities of anode slurries decreased on addition of low TNFC levels but began to increase at a TNFC concentration of 0.1% (Fig. 4(a) and (b)). It is difficult to disperse hydrophobic graphite particles in aqueous phase without a dispersion agent. However, TNFC in a certain crystal phase are amphiphilic and can thus be used to disperse graphite. Indeed, due to their amphiphilic nature, NFC have been used as stabilizers for various hydrophobic particles in previous studies (Olivier *et al.* 2012; Koga *et al.* 2013; Hamedi *et al.* 2014; Zhang *et al.* 2017).

Initially, TNFC interact with the graphite surfaces, improving dispersion and decreasing the viscosity. However, beyond a certain level, unattached TNFC in a slurry form a TNFC network and acts as a thickener, increasing viscosity. Although the viscosity

was lowest at a TNFC concentration of 0.1%, this does not indicate that particle dispersion was optimal. Figure 4(e) shows the enhanced particle dispersion with the addition of TNFC, and the further improvement in dispersion at higher TNFC concentrations (1.5%). Therefore, initially, TNFC were primarily absorbed to graphite surfaces *via* hydrophobic interactions, but with the addition of more TNFC, TNFC in the slurry and those attached to graphite surfaces interact to form a network, as reported previously (Oh *et al.* 2021). This ultimately improves particle dispersion and increases the slurry viscosity.

Achieving uniform particle dispersion is critical for forming a homogeneous structure with uniform pore distribution in the anode layer. The uniformity of the structure not only influences the mechanical strength of the layer but is also strongly correlated with battery swelling and volumetric expansion. A consistent pore size and distribution within the electrode can effectively mitigate the stress generated during charging and discharging cycles, acting as a buffer against volume change (Yi *et al.* 2013a,b; Tian *et al.* 2015; Park *et al.* 2019; Lee *et al.* 2020). Thus, the improved dispersion facilitated by the introduction of TNFC as binders is expected to enhance battery performance by better controlling volume expansion. A similar trend was observed in CMC–graphite anode slurries. The viscosity initially decreased with CMC addition, but it began to increase after the CMC concentration reached 0.2%, as seen with the TNFC–graphite anode slurries. However, the viscosity increases of CMC-containing slurries were much lower than those of slurries with TNFC; the thickening mechanisms were quite different. A more detail discussion is provided through the observation of viscoelastic behavior of anode slurries.

The viscoelastic behaviors of anode slurries with TNFC were investigated using oscillatory tests (Fig. 5). The storage modulus ( $G'$ ) indicates the solid-like elastic behavior of a slurry, and the loss modulus ( $G''$ ) indicates liquid-like viscous behavior. In the amplitude tests, the slurries exhibited linear viscoelastic regions until the yield strains were reached, at which time  $G'$  began to decrease; this indicated the beginning of structural breakdown (Fig. 5(a) and (c)). Compared to slurries with TNFC, those with CMC exhibited higher yield strains and less variation among different binder concentrations. However,  $G'$  was higher in slurries with TNFC, suggesting that the structures were more solid-like. This suggestion was supported by comparison of  $G'$  and  $G''$ ; slurries with CMC exhibited a higher  $G''$  than  $G'$ , with slurries having TNFC showing the reverse.

The frequency sweep test at fixed strain also revealed different tendencies between TNFC and CMC anode slurries (Fig. 5(b) and (d)). The  $G'$  and  $G''$  of TNFC anode slurries did not change significantly as the frequency increased, whereas those of CMC anode slurries gradually increased; this indicated that TNFC formed stronger structures than CMC with the different mechanisms of slurry–binder interactions and structure formation.

Excess CMC molecules that are not adsorbed onto graphite increase the viscosity of an anode slurry *via* CMC molecular entanglement. This entanglement of CMC molecules does not cause flocculation of graphite particles, resulting in the slurry behaving like liquid (Lim *et al.* 2015). In contrast, TNFC exhibit higher aspect ratios and more accessible hydrophobic backbones than CMCs with carboxymethyl substitutes (Moon *et al.* 2011; Medronho *et al.* 2012; Lindman *et al.* 2017), but TNFC have fewer functional groups that induce electrostatic repulsion, as only C6 position is functionalized during TEMPO-oxidation (Isogai *et al.* 2011). Thus, TNFC could form stronger structures than CMCs by interacting with graphite and creating rigid, solid-like network structures even at higher TNFC concentrations.

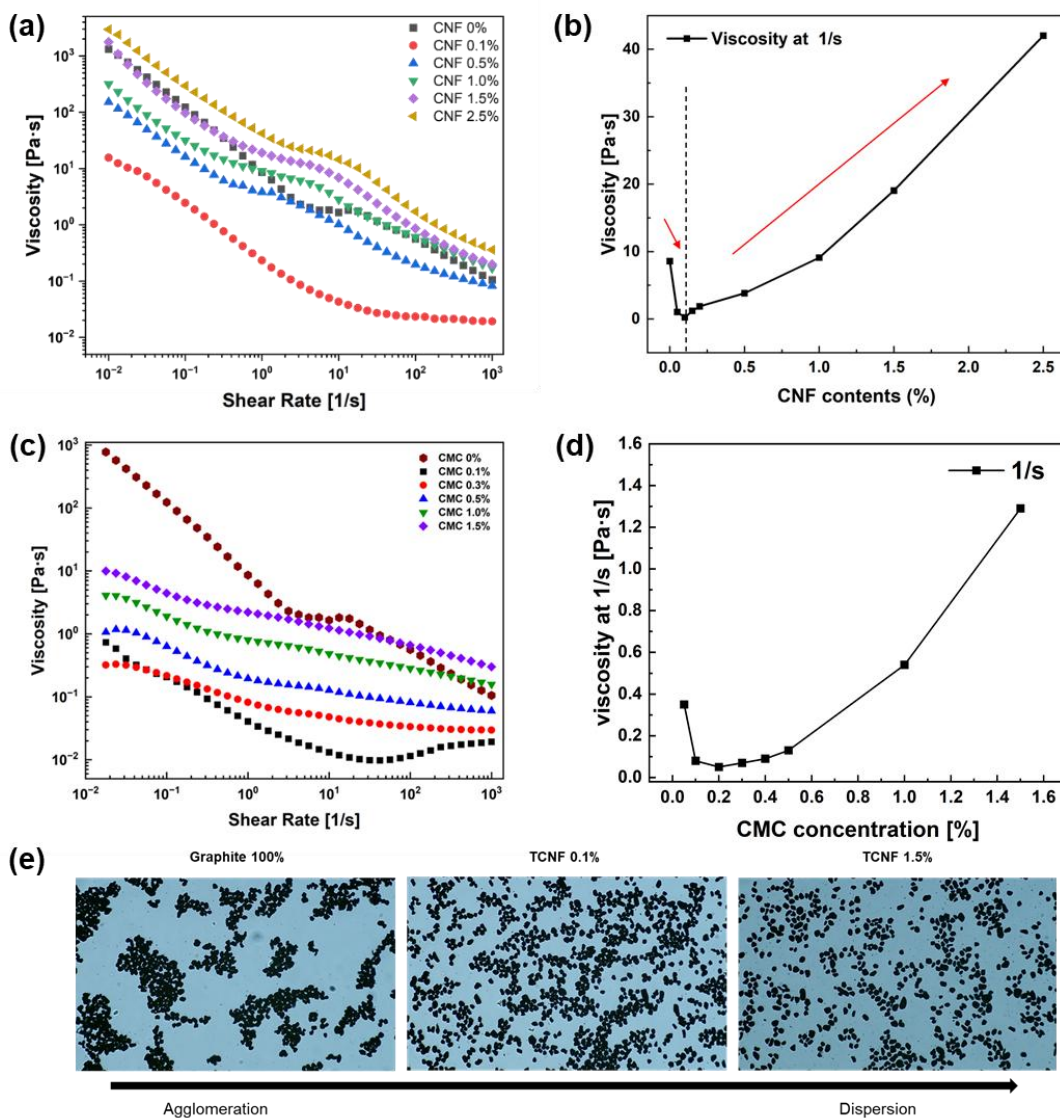


**Fig. 4.** The viscosities of anode slurries with TNFC (a, b) and CMC (c, d) and optical micrographs of the slurries (e). (a) and (c): Viscosities of anode slurries as a function of shear rate. (b) and (d): Viscosities of anode slurries as a function of TNFC and CMC contents. (e): Anode slurries with different TNFC concentrations. These slurries were diluted 30-fold from the original slurries with 50% solid content. Images were taken 60 s after dropping, and particle stability was evaluated.



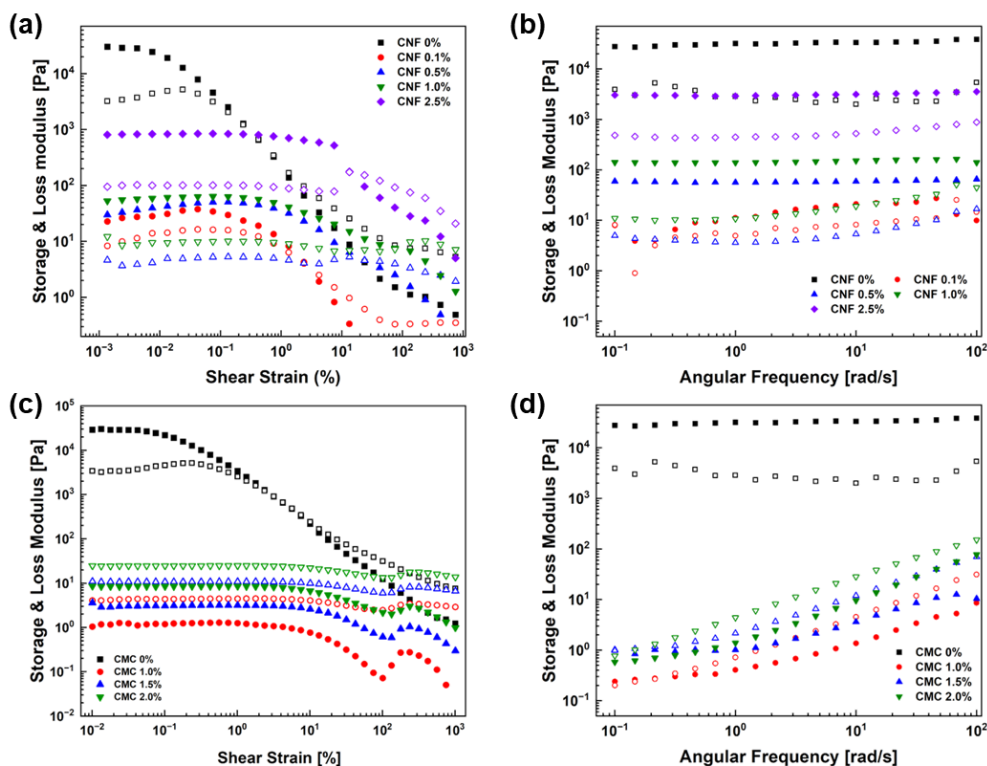


**Fig. 5.** Storage ( $G'$ ) and loss ( $G''$ ) moduli of anode slurries with TNFC (a, b) and CMC (c, d). (a) and (c): Moduli measured using amplitude sweep tests ( $G'$  and  $G''$  versus shear strain (%); Solid symbols:  $G'$ ; hollow symbols:  $G''$ ). (b) and (d): Moduli measured using frequency sweep tests ( $G'$  and  $G''$  versus angular frequency (rad/s); Solid symbols:  $G'$ ; hollow symbols:  $G''$ ).

The solid-like structure is beneficial to the structural stability during the electrode fabrication process and performance. The higher storage modulus ( $G'$ ) indicate that they behave more like solids, which means they can better maintain their structure under stress during processes such as coating and drying (Nardo and Farè 2017; Chung 2019; Ansari *et al.* 2021). This solid-like behavior helps prevent particle aggregation and settling, leading to more uniform layers with consistent pore distribution (Bao *et al.* 2024). Additionally, solid-like behavior can improve the mechanical strength of the electrode, making it more resilient to cracking or deformation during manufacturing process, thus enhancing the overall durability and performance of the battery. The fact that slurries with TNFC exhibited more solid-like behavior suggests that the TNFC contributed to the formation of a more robust, stable structure that can better withstand the mechanical and electrochemical stresses encountered during battery operation.

### Mechanical Properties of Anode Layers with TNFC

The effects of TNFC on mechanical properties were investigated in terms of anode adhesion to a layer of copper foil and the tensile strength of anode free-standing composites. Adhesion was reflected by the layer peel strength in the 90° peel test (Fig. 2). Anode layers with conventional SBR and CMC binders were also evaluated as references (Table 1). Figure 6 shows the results. The average peel strength was calculated based on measurements obtained at peel distances of 5 to 30 mm (Table 2). Overall, compared to the references, the peel strength fell significantly when TNFC served as the anode binders, although increased TNFC concentrations slightly improved the peel strength.

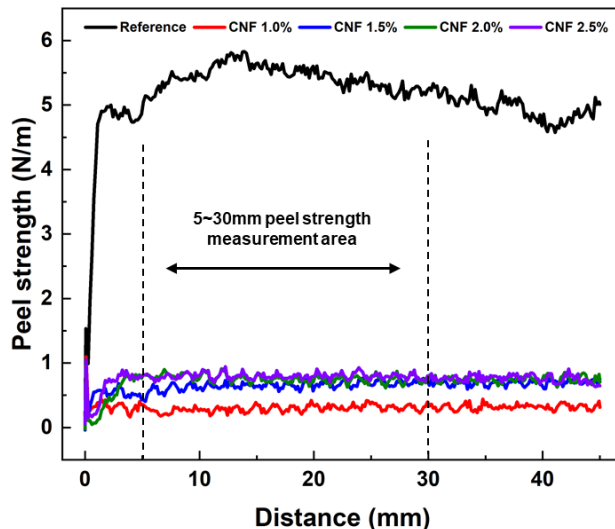


**Fig. 6.** Peel strength of anode layers on copper foil

**Table 2.** Average Peel Strength of Anode Layers Derived from Measurements Obtained at Peel Distances of 5 to 30 mm (Fig. 6)

| Condition | Peel Strength (N/m) |
|-----------|---------------------|
| Reference | 5.26 ± 0.30         |
| TNFC 1.0% | 0.28 ± 0.07         |
| TNFC 1.5% | 0.64 ± 0.10         |
| TNFC 2.0% | 0.65 ± 0.10         |
| TNFC 2.5% | 0.80 ± 0.10         |

Note: The values are means ± standard deviations.

The adhesion of anode layers to foil was further analyzed by examining the foil after the peel test (Fig. 7). The surfaces of reference layers (anodes with SBR and CMC) were dark black after the test, but that of the anode layer with the TNFC binders showed the copper surface; little of the black graphite anode remained, indicating reduced adhesion of the anode layer. Optical microscopy revealed fewer graphite particles on the copper surface when TNFC were used. Such low adhesion of anode layers with TNFC must be improved for practical applications.

The lower adhesion of anode layers with TNFC might be attributed to their hydrophilic nature. Although TNFC exhibit partial amphiphilic properties with hydrophobic planes, they still possess abundant hydroxyl groups, making the layer more polar. In contrast, SBR contains styrene and butadiene components that interact more effectively with non-polar surfaces like copper, and its lower surface energy enhances its ability to spread across the copper surface (Martín-Martínez 2002; Zempel 2006; Sisanth *et al.* 2017). Indeed, in the SBR/CMC binder system, it was reported that anodes without SBR exhibited very low adhesion (Hofmann *et al.* 2024), underscoring the crucial role of SBR in adhesion to copper. To improve the adhesion of TNFC binders to copper, the incorporation of SBR with TNFC, or other adhesion-enhancing materials such as poly(acrylic acid) (Lee *et al.* 2006), or surface treatments of copper foil, such as wet chemical and plasma treatments, could be considered (Turunen and Kivilahti 2003; Borges *et al.* 2009). These approaches warrant further study to optimize the use of TNFC as a binder.

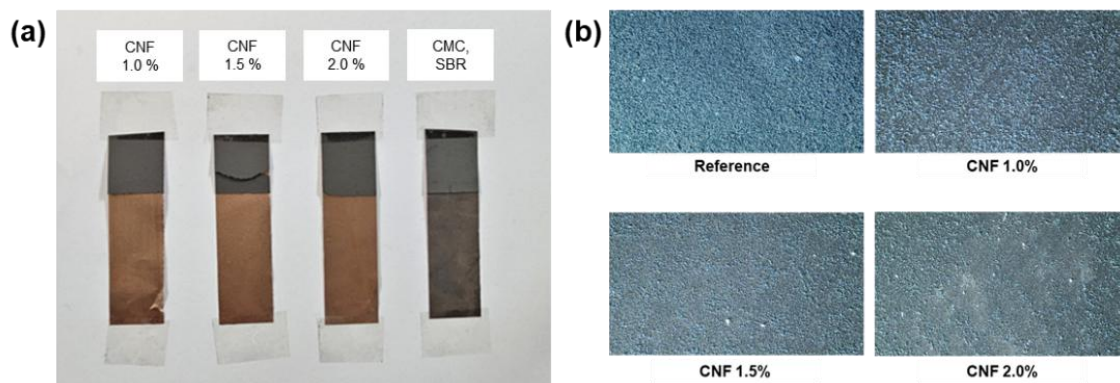


**Fig. 7.** Copper foil surface analysis after the peel test. (a): The copper foils after the test and (b): microscopic images of the copper foil surfaces after the peel test

TNFC binders greatly improved the tensile stress of anode composites, despite the fact that adhesion decreased (Fig. 8 and Table 3). When TNFC were added up to 1.5%, the tensile stress and strain at yield were lower than those of the reference samples. However, beginning at 2.0% TNFC, the tensile stress of the anode composite improved significantly to surpass those of the references, aligning with previous findings on improved shear strength (Françon *et al.* 2022). While in the previous study the TNFC content in the slurry was 5%, and the reference condition for SBR/CMC was 2.5%/2.5%, the current study used a lower binder content in the TNFC samples compared to the reference, yet still achieved higher tensile stress. Specifically, TNFC at 2.0% was associated with a strain at yield comparable to those of the references, but also with improved tensile stress; this was attributed to enhanced graphite particle dispersity and network formation between free and particle-attached TNFC, yielding uniform structures that reduced failure at weak points within layers. Such networks would be expected to enhance anode dimensional stability by minimizing anode expansion during discharging and charging.

Strain at break is a crucial parameter for anode materials, as it reflects the material's ability to withstand deformation under mechanical stress without fracturing. A higher strain at break indicates that the anode material can better accommodate the mechanical strains that occur during battery cycling, thereby enhancing its durability and extending its operational lifespan. In this study, the reference material demonstrated the highest strain at break, highlighting its inherent flexibility despite its lower tensile strength. Given the higher elongation of CMC films compared to TNFC films, the reduction in elongation with TNFC is reasonable (Oun and Rhim 2015; Françon *et al.* 2022). In contrast, TNFC-reinforced composites at concentrations of 2.0% and 2.5% exhibited significantly increased tensile strength. Notably, the 2.0% TNFC sample maintained a strain at break comparable to that of the reference, indicating that this concentration strikes an optimal balance. This balance between tensile strength and strain at break at 2.0% TNFC suggests that the material is sufficiently reinforced to improve mechanical properties while retaining enough flexibility to avoid brittle failure.

Toughness, representing the total energy absorbed by the material before fracture, further supports this conclusion. The 2.0% TNFC sample achieved the highest toughness of 12,200 J/m<sup>3</sup>, reflecting its ability to combine tensile strength with strain at break effectively. Although the 2.5% TNFC sample showed a higher tensile strength, its toughness decreased slightly to 9,700 J/m<sup>3</sup>, indicating increased brittleness at this concentration. These findings highlight the finding that the 2.0% TNFC concentration not

only optimizes tensile strength and strain at break but also maximizes toughness, making it the most promising candidate for enhancing the mechanical durability of anode materials.

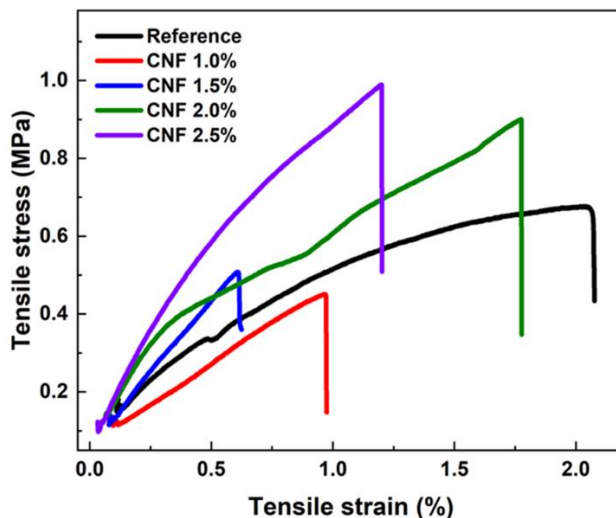


**Fig. 8.** Tensile stress of anode free-standing composites

**Table 3.** Average Tensile Stress and Strain at Yield of Anode Free-standing Composites

| Condition | Tensile stress (MPa) | Strain at break (%) | Toughness (J/m <sup>3</sup> ) |
|-----------|----------------------|---------------------|-------------------------------|
| Reference | 0.72 ± 0.04          | 2.19 ± 0.28         | 10,200                        |
| TNFC 1.0% | 0.42 ± 0.06          | 1.10 ± 0.44         | 2,900                         |
| TNFC 1.5% | 0.56 ± 0.09          | 0.61 ± 0.28         | 1,700                         |
| TNFC 2.0% | 0.86 ± 0.11          | 1.91 ± 0.26         | 12,200                        |
| TNFC 2.5% | 0.95 ± 0.16          | 1.18 ± 0.45         | 9,700                         |

Note: The tensile tests were conducted five times, and means with standard deviations were calculated.

This study explored the potential of TNFC as an anode binder through its impact on the rheological and mechanical properties of anode slurries and the electrode layer. TNFC, with better mechanical properties and network-forming capacity than conventional binders such as SBR and CMC, may be valuable as future anode binders. However, in practical terms, the low level of TNFC adhesion to copper foil must be improved. Combining TNFC with SBR or pretreating the copper surface may solve this issue; further study is required. Future research will also focus on anode layer stability after discharging/charging, *i.e.*, dimensional changes and the extent of defect generation, to optimize TNFC as anode binders.

## CONCLUSIONS

1. TEMPO-oxidized nanofibrillated cellulose (TNFC), a renewable and environmentally friendly material, can serve as a new anode binder that address failures associated with volumetric expansion during the charging/discharging of lithium-ion batteries.
2. The TNFC binder mechanism differs from that of conventional carboxymethyl cellulose (CMC) binders, resulting in stronger and more elastic structures. TNFC



particles interact directly with graphite and form networks between graphite-attached and free TNFC.

3. TNFC was found to enhance the mechanical properties of conventional anode composites by improving graphite particle dispersion and by serving as a thickener that created uniform anode structures.
4. An anode slurry with 2.0% TNFC content demonstrated superior tensile stress and elongation, thereby improving the toughness of the anode layer.

## ACKNOWLEDGMENTS

This work was financially supported by National Research Foundation of Korea (Grant No. RS-2022-NR072240) and LG Energy Solution.

## REFERENCES CITED

- Ansari, I. A., Gupta, G. A., Ramkumar, J., and Kar, K. K. (2021). "22 - Fly ash-mixed polymeric media for abrasive flow machining process," in: *Handbook of Fly Ash*, K. K. Kar (ed.), Butterworth-Heinemann, 681-713. DOI: 10.1016/B978-0-12-817686-3.00003-7
- Bao, Z., Zhu, H., Wang, Y., and Chang, Q. (2024). "A new method for judging and predicting the stability of ceramic suspensions by rheological tests," *Colloids and Surfaces A: Physicochemical and Engineering Aspects*, 685, article 133316. DOI: 10.1016/j.colsurfa.2024.133316
- Borges, J. N., Belmonte, T., Guillot, J., Duday, D., Moreno-Couranjou, M., Choquet, P., and Migeon, H.-N. (2009). "Functionalization of copper surfaces by plasma treatments to improve adhesion of epoxy resins," *Plasma Processes and Polymers*, 6(S1), S490-S495. DOI: 10.1002/ppap.200931106
- Buqa, H., Holzapfel, M., Krumeich, F., Veit, C., and Novák, P. (2006). "Study of styrene butadiene rubber and sodium methyl cellulose as binder for negative electrodes in lithium-ion batteries," *Journal of Power Sources*, 161(1), 617-622. DOI: 10.1016/j.jpowsour.2006.03.073
- Chung, D. D. L. (2019). "Interface-derived solid-state viscoelasticity exhibited by nanostructured and microstructured materials containing carbons or ceramics," *Carbon*, 144, 567-581. DOI: 10.1016/j.carbon.2018.12.097
- De Nardo, L., and Farè, S. (2017). "9 - Dynamic-mechanical characterization of polymer biomaterials," in: *Characterization of Polymeric Biomaterials*, M. C. Tanzi and S. Farè (eds.), Woodhead Publishing, pp. 203-232. DOI: 10.1016/B978-0-08-100737-2.00009-1
- Dimic-Misic, K., Gane, P. A. C., and Paltakari, J. (2013). "Micro- and nanofibrillated cellulose as a rheology modifier additive in CMC-containing pigment-coating formulations," *Industrial & Engineering Chemistry Research* 52(45), 16066-16083. DOI: 10.1021/ie4028878
- Dufficy, M. K., Corder, R. D., Dennis, K. A., Fedkiw, P. S., and Khan, S. A. (2021). "Guar gel binders for silicon nanoparticle anodes: Relating binder rheology to electrode performance," *ACS Applied Materials & Interfaces* 13(43), 51403-51413.

- DOI: 10.1021/acsami.1c10776
- El Kharbachi, A., Zavorotynska, O., Latroche, M., Cuevas, F., Yartys, V., and Fichtner, M. (2020). “Exploits, advances and challenges benefiting beyond Li-ion battery technologies,” *Journal of Alloys and Compounds* 817, article 153261. DOI: 10.1016/j.jallcom.2019.153261
- Fernández-Santos, J., Valls, C., Cusola, O., and Roncero, M. B. (2022). “Composites of cellulose nanocrystals in combination with either cellulose nanofibril or carboxymethylcellulose as functional packaging films,” *International Journal of Biological Macromolecules* 211, 218-229. DOI: 10.1016/j.ijbiomac.2022.05.049
- Françon, H. S., Gorur, Y. C., Montanari, C., Larsson, P. A., and Wågberg, L. (2022). “Toward Li-ion graphite anodes with enhanced mechanical and electrochemical properties using binders from chemically modified cellulose fibers,” *ACS Applied Energy Materials* 5(8), 9333-9342. DOI: 10.1021/acsaem.2c00525
- Ge, J., Turunen, M. P. K., and Kivilahti, J. K. (2003). “Surface modification and characterization of photodefinable epoxy/copper systems,” *Thin Solid Films*, 440(1), 198-207. DOI: 10.1016/S0040-6090(03)00851-4
- Gordon, R., Kassar, M., and Willenbacher, N. (2020a). “Effect of polymeric binders on dispersion of active particles in aqueous LiFePO<sub>4</sub>-based cathode slurries as well as on mechanical and electrical properties of corresponding dry layers,” *ACS Omega* 5(20), 11455-11465. DOI: 10.1021/acsomega.0c00477
- Gordon, R., Orias, R., and Willenbacher, N. (2020b). “Effect of carboxymethyl cellulose on the flow behavior of lithium-ion battery anode slurries and the electrical as well as mechanical properties of corresponding dry layers,” *Journal of Materials Science* 55(33), 15867-15881. DOI: 10.1007/s10853-020-05122-3
- Hamedi, M. M., Hajian, A., Fall, A. B., Håkansson, K., Salajkova, M., Lundell, F., Wågberg, L., and Berglund, L. A. (2014). “highly conducting, strong nanocomposites based on nanocellulose-assisted aqueous dispersions of single-wall carbon nanotubes,” *ACS Nano* 8(3), 2467-2476. DOI: 10.1021/nn4060368
- Hochgatterer, N. S., Schweiger, M. R., Koller, S., Raimann, P. R., Wöhrle, T., Wurm, C., and Winter, M. (2008). “Silicon/graphite composite electrodes for high-capacity anodes: Influence of binder chemistry on cycling stability,” *Electrochemical and Solid-State Letters* 11(5), A76. DOI: 10.1149/1.2888173
- Hofmann, K., Hegde, A. D., Liu-Theato, X., Gordon, R., Smith, A., and Willenbacher, N. (2024). “Effect of mechanical properties on processing behavior and electrochemical performance of aqueous processed graphite anodes for lithium-ion batteries,” *Journal of Power Sources* 593, article 233996. DOI: 10.1016/j.jpowsour.2023.233996
- Isogai, A., Saito, T., and Fukuzumi, H. (2011). “TEMPO-oxidized cellulose nanofibers,” *Nanoscale* 3(1), 71-85. DOI: 10.1039/C0NR00583E
- Iwamoto, S., Kai, W., Isogai, A., and Iwata, T. (2009). “Elastic modulus of single cellulose microfibrils from tunicate measured by atomic force microscopy,” *Biomacromolecules* 10(9), 2571-2576. DOI: 10.1021/bm900520n
- Iwamoto, S., Lee, S.-H., and Endo, T. (2014). “Relationship between aspect ratio and suspension viscosity of wood cellulose nanofibers,” *Polymer Journal* 46(1), 73-76. DOI: 10.1038/pj.2013.64
- Kitamura, K., Tanaka, M., and Mori, T. (2022). “Effects of the mixing sequence on the graphite dispersion and resistance of lithium-ion battery anodes,” *Journal of Colloid and Interface Science* 625, 136-144. DOI: 10.1016/j.jcis.2022.06.006
- Koga, H., Saito, T., Kitaoka, T., Nogi, M., Suganuma, K., and Isogai, A. (2013).

- “Transparent, conductive, and printable composites consisting of tempo-oxidized nanocellulose and carbon nanotube,” *Biomacromolecules* 14(4), 1160-1165. DOI: 10.1021/bm400075f
- Lee, D., Kondo, A., Lee, S., Myeong, S., Sun, S., Hwang, I., Song, T., Naito, M., and Paik, U. (2020). “Controlled swelling behavior and stable cycling of silicon/graphite granular composite for high energy density in lithium ion batteries,” *Journal of Power Sources* 457, article 228021. DOI: 10.1016/j.jpowsour.2020.228021
- Lee, J. H., Lee, H. M., and Ahn, S. (2003). “Battery dimensional changes occurring during charge/discharge cycles—Thin rectangular lithium ion and polymer cells,” *Journal of Power Sources*, Selected papers presented at the 11<sup>th</sup> International Meeting on Lithium Batteries, 119–121, 833-837. DOI: 10.1016/S0378-7753(03)00281-7
- Lee, J.-H., Paik, U., Hackley, V. A., and Choi, Y.-M. (2006). “Effect of poly(acrylic acid) on adhesion strength and electrochemical performance of natural graphite negative electrode for lithium-ion batteries,” *Journal of Power Sources* 161(1), 612-616. DOI: 10.1016/j.jpowsour.2006.03.087
- Lim, S., Kim, S., Ahn, K. H., and Lee, S. J. (2015). “The effect of binders on the rheological properties and the microstructure formation of lithium-ion battery anode slurries,” *Journal of Power Sources* 299, 221-230. DOI: 10.1016/j.jpowsour.2015.09.009
- Lindman, B., Medronho, B., Alves, L., Costa, C., Edlund, H., and Norgren, M. (2017). “The relevance of structural features of cellulose and its interactions to dissolution, regeneration, gelation and plasticization phenomena,” *Physical Chemistry Chemical Physics* 19(35), 23704-23718. DOI: 10.1039/C7CP02409F
- Lu, H., Guccini, V., Kim, H., Salazar-Alvarez, G., Lindbergh, G., and Cornell, A. (2017). “Effects of different manufacturing processes on TEMPO-oxidized carboxylated cellulose nanofiber performance as binder for flexible lithium-ion batteries,” *ACS Applied Materials & Interfaces* 9(43), 37712-37720. DOI: 10.1021/acsami.7b10307
- Martín-Martínez, J. M. (2002). “Chapter 13 - Rubber base adhesives,” in: *Adhesion Science and Engineering*, D. A. Dillard, A. V. Pocius, and M. Chaudhury (eds.), Elsevier Science B.V., Amsterdam, 573-675. DOI: 10.1016/B978-044451140-9/50013-5
- Medronho, B., Romano, A., Miguel, M. G., Stigsson, L., and Lindman, B. (2012). “Rationalizing cellulose (in)solubility: Reviewing basic physicochemical aspects and role of hydrophobic interactions,” *Cellulose* 19(3), 581-587. DOI: 10.1007/s10570-011-9644-6
- Moon, R., Martini, A., Nairn, J., Simonsen, J., and Youngblood, J. (2011). “Cellulose nanomaterials review: Structure, properties and nanocomposites,” *Chemical Society Reviews* 40(7), 3941-3994. DOI: 10.1039/C0CS00108B
- Nirmale, T. C., Kale, B. B., and Varma, A. J. (2017). “A review on cellulose and lignin based binders and electrodes: Small steps towards a sustainable lithium ion battery,” *International Journal of Biological Macromolecules* 103, 1032-1043. DOI: 10.1016/j.ijbiomac.2017.05.155
- Nitta, N., Wu, F., Lee, J. T., and Yushin, G. (2015). “Li-ion battery materials: Present and future,” *Materials Today* 18(5), 252-264. DOI: 10.1016/j.mattod.2014.10.040
- Nirmale, T. C., Kale, B. B., and Varma, A. J. (2017). “A review on cellulose and lignin based binders and electrodes: Small steps towards a sustainable lithium ion battery,” *International Journal of Biological Macromolecules* 103, 1032-1043. DOI: 10.1016/j.ijbiomac.2017.05.155

- Oh, K., Lee, J.-H., Im, W., Rajabi Abhari, A., and Lee, H. L. (2017). "Role of cellulose nanofibrils in structure formation of pigment coating layers," *Industrial & Engineering Chemistry Research* 56(34), 9569-9577. DOI: 10.1021/acs.iecr.7b02750
- Oh, K., Shen, Z., Kwon, S., and Toivakka, M. (2021). "Thermal properties of graphite/salt hydrate phase change material stabilized by nanofibrillated cellulose," *Cellulose* 28(11), 6845-6856. DOI: 10.1007/s10570-021-03936-1
- Olivier, C., Moreau, C., Bertoncini, P., Bizot, H., Chauvet, O., and Cathala, B. (2012). "Cellulose nanocrystal-assisted dispersion of luminescent single-walled carbon nanotubes for layer-by-layer assembled hybrid thin films," *Langmuir* 28(34), 12463-12471. DOI: 10.1021/la302077a
- Oun, A. A., and Rhim, J.-W. (2015). "Preparation and characterization of sodium carboxymethyl cellulose/cotton linter cellulose nanofibril composite films," *Carbohydrate Polymers* 127, 101-109. DOI: 10.1016/j.carbpol.2015.03.073
- Park, K., Myeong, S., Shin, D., Cho, C.-W., Kim, S. C., and Song, T. (2019). "Improved swelling behavior of Li ion batteries by microstructural engineering of anode," *Journal of Industrial and Engineering Chemistry* 71, 270-276. DOI: 10.1016/j.jiec.2018.11.035
- Qian, J., Chen, Y., Wu, L., Cao, Y., Ai, X., and Yang, H. (2012). "High capacity Na-storage and superior cyclability of nanocomposite Sb/C anode for Na-ion batteries," *Chemical Communications* 48(56), 7070-7072. DOI: 10.1039/C2CC32730A
- Qiu, L., Shao, Z., Liu, M., Wang, J., Li, P., and Zhao, M. (2014). "Synthesis and electrospinning carboxymethyl cellulose lithium (CMC-Li) modified 9,10-anthraquinone (AQ) high-rate lithium-ion battery," *Carbohydrate Polymers* 102, 986-992. DOI: 10.1016/j.carbpol.2013.09.105
- Rautkoski, H., Pajari, H., Koskela, H., Sneck, A., and Moilanen, P. (2015). "Use of cellulose nanofibrils (NFC) in coating colors," *Nordic Pulp & Paper Research Journal* 30(3), 511-518. DOI: 10.3183/npprj-2015-30-03-p511-518
- Salo, T., Dimic-Misic, K., Gane, P., and Paltakari, J. (2015). "Application of pigmented coating colours containing MFC/NFC: Coating properties and link to rheology," *Nordic Pulp & Paper Research Journal* 30(1), 165-178. DOI: 10.3183/npprj-2015-30-01-p165-178
- Schweidler, S., de Biasi, L., Schiele, A., Hartmann, P., Brezesinski, T., and Janek, J. (2018). "Volume changes of graphite anodes revisited: A combined operando X-ray diffraction and *in situ* pressure analysis study," *The Journal of Physical Chemistry C* 122(16), 8829-8835. DOI: 10.1021/acs.jpcc.8b01873
- Sen, U. K., and Mitra, S. (2013). "High-rate and high-energy-density lithium-ion battery anode containing 2D MoS<sub>2</sub> nanowall and cellulose binder," *ACS Applied Materials & Interfaces* 5(4), 1240-1247. DOI: 10.1021/am3022015
- Sisanth, K. S., Thomas, M. G., Abraham, J., and Thomas, S. (2017). "1 - General introduction to rubber compounding," in: *Progress in Rubber Nanocomposites*, Woodhead Publishing Series in Composites Science and Engineering, S. Thomas and H. J. Maria (eds.), Woodhead Publishing, pp. 1-39. DOI: 10.1016/B978-0-08-100409-8.00001-2
- Tian, H., Tan, X., Xin, F., Wang, C., and Han, W. (2015). "Micro-sized nano-porous Si/C anodes for lithium ion batteries," *Nano Energy*, 11, 490-499. DOI: 10.1016/j.nanoen.2014.11.031
- Wassiliadis, N., Schneider, J., Frank, A., Wildfeuer, L., Lin, X., Jossen, A., and Lienkamp, M. (2021). "Review of fast charging strategies for lithium-ion battery



- systems and their applicability for battery electric vehicles,” *Journal of Energy Storage* 44, article 103306. DOI: 10.1016/j.est.2021.103306
- Yi, R., Dai, F., Gordin, M. L., Chen, S., and Wang, D. (2013a). “Micro-sized Si-C composite with interconnected nanoscale building blocks as high-performance anodes for practical application in lithium-ion batteries,” *Advanced Energy Materials* 3(3), 295-300. DOI: 10.1002/aenm.201200857
- Yi, R., Dai, F., Gordin, M. L., Sohn, H., and Wang, D. (2013b). “Influence of silicon nanoscale building blocks size and carbon coating on the performance of micro-sized Si-C composite Li-Ion anodes,” *Advanced Energy Materials* 3(11), 1507-1515. DOI: 10.1002/aenm.201300496
- Zhang, X., Lu, Z., Zhao, J., Li, Q., Zhang, W., and Lu, C. (2017). “Exfoliation/dispersion of low-temperature expandable graphite in nanocellulose matrix by wet co-milling,” *Carbohydrate Polymers* 157, 1434-1441. DOI: 10.1016/j.carbpol.2016.11.023

Article submitted: July 7, 2024; Peer review completed: August 7, 2024; Revised version received: August 19, 2024; Accepted: March 4, 2025; Published: April 1, 2025.  
DOI: 10.15376/biores.20.2.3732-3748